Combining imaging sonar and photogrammetry for underwater object localization and mapping

Michael Grömer [1, 2], Benjamin Wild [2], Camillo Ressl [2], Johannes Otepka [2], Gottfried Mandlburger [2]

[1] Verbund Hydro Power GmbH, Vienna, Austria
[2] Department of Geodesy and Geoinformation, TU Wien, Vienna, Austria
michael.groemer@verbund.com; (benjamin.wild, camillo.ressl, johannes.otepka, gottfried.mandlburger) @geo.tuwien.ac.at

Keywords: ROV, Underwater Measurement, Photogrammetry, Imaging Sonar, Sensor Combination,

Abstract

During the flooding event in September 2024 in Austria, an unknown number of industrial barrels was washed into a freshwater pond near Loosdorf, leading to this study aimed at locating and measuring these barrels. Due to significant turbidity, with a Secchi depth of 1.1 m, traditional airborne inspection methods failed to locate the barrels. Consequently, we employed a Remotely Operated Vehicle (ROV), equipped with various sensors including an imaging sonar Oculus M3000d, a 4K camera, and a laser scaler. Using the imaging sonar, we successfully identified twelve barrels within a study area exceeding one hectare. After identifying the barrels, our goal was to determine the dimensions (height and diameter) of the barrels. While visibility limitations restricted photogrammetric evaluations, sonar data allowed accurate height measurements. However, the diameter could not be determined using the imaging sonar, so that the camera and laser scaler were employed for this task. Despite challenges posed by turbidity, the combination of these sensors proved effective for this case of underwater inspections. The objects were found, and the dimensions could be determined. This study demonstrates the potential of combining imaging sonar, cameras, and laser scaling techniques in underwater environments, particularly under low visibility conditions.

1. Introduction

1.1 General Introduction

Remote sensing of underwater objects plays an important role in many disciplines such as underwater engineering and maintenance, defence operations, archaeology and marine science studies (Parnum et al., 2024). Multibeam sonar (Sound Navigation And Ranging) systems can be categorized primarily into two types: bathymetric and imaging systems. Bathymetric multibeam sonar systems, also known as multibeam echosounders, are specifically designed to measure water depth. They feature a narrow azimuth angle (typically 0.5–2°) and are oriented towards the seafloor (Lurton et al., 2010). In contrast, imaging sonar systems aim to visualize the underwater environment; they are typically deployed horizontally and have a larger receiver azimuth angle (approximately 10–30°) than bathymetric systems (Song et al., 2016).

Multibeam sonar systems are sophisticated underwater mapping devices that function by emitting sound waves through an acoustic projector. The transmitted sound operates over a wide opening angle of 120° to 180°, while maintaining a narrower azimuth swath of 0.5° to 30°. Upon transmission, the system captures the acoustic energy that is scattered back to the sonar, a phenomenon known as backscattering, using an array of receivers. The determination of the angle of backscatter is achieved through electronic beamforming techniques. Additionally, the range to the reflecting surface is calculated using the two-way travel time of the emitted sound waves (Lurton et al., 2010).

Multibeam sonar systems can be deployed on different carrier platforms, for example, remotely operated underwater vehicle (ROVs), vessels and autonomous underwater vehicles (AUVs). We used an ROV as carrier platform (Deeptrekker, 2025).

1.2 Experimental Setup

During the flooding event in Austria in September 2024, an unknown number of industry barrels was flushed into a freshwater pond near Loosdorf (Lower Austria). This situation and the search for these barrels led to our research questions:

- Is it possible to determine the number and location of the barrels?
- Can we determine the dimensions (height and diameter) of the barrels?

Because of the significant turbidity with a Secchi depth of 1.1 m in this pond, airborne inspections methods failed to locate and map the barrels. In scenarios where water clarity is insufficient for the visual identification and accurate measurement of targets, acoustic techniques are frequently employed as alternatives for remote sensing in aquatic environments (Demer et al., 2015). For that reason, we decided to use a ROV equipped with multiple sensors for this task (Chemisky et al., 2021). Our idea was to combine the various sensors on board the ROV and to make use of the abilities we gained trough this combination to answer our research questions. The employed ROV was a Deep Trekker Revolution which was equipped with the following sensors:

- Imaging Sonar Oculus M3000d (Blueprint, 2025)
- 4k camera (Sony)
- Laser scaler
- Doppler Velocity Log (DVL)
- Depth-, temperature sensor, compass
- Inertial Measurement Unit (IMU)

The challenge was the lack of information (unknown number or position of the barrels) and the high turbidity. The imaging sonar is an excellent option to look for specific objects (Sun et al., 2016; Sun et al., 2021). One major application of imaging sonars is fish monitoring (Wei et al., 2022). The imaging sonars accuracy and precision during the measurement of small-bodied fish was investigated by Cook et al. (2019). The accuracies of the sonar system are also analysed in detail in Helminen et al. (2020), the accuracy of length measurements with the Oculus M3000d imaging sonar was analyzed by Parnum et al. (2024).

1.3 Combined Use of Sonar Systems and Underwater Cameras in Literature

The combination of sonar and camera has been used for many different applications, in the following section some applications are presented, e.g., improved underwater localization and mapping, where the authors were using the complimentary properties of sonars and cameras to improve underwater visual odometry and point cloud generation (Cardaillac et al., 2015). The authors concluded that this task remains difficult as the image generation concepts are different, giving challenges to direct acoustic and optic feature matching.
A two-step inspection approach that combines sonar, camera, and deep learning to enable rapid and accurate underwater bridge pier inspections was created to improve ROV inspections of infrastructure (Sun et al., 2025).

Imaging sonar and underwater camera data were used together in a novel method to estimate the sizes of different salmon species populations. Fish recorded by sonar were categorized based on species proportions derived from underwater camera data, enhancing the accuracy of population assessments by leveraging the strengths of both technologies (Helminen et al., 2023).

The combination of sonar and camera systems also proved useful in sea floor mapping. Towed camera systems are commonly used to capture images of the deep seafloor for research and management purposes, but their optical surveys are limited by the rapid attenuation of visible wavelengths in water. By using an advanced towed platform that combines imaging cameras with acoustic devices, the effectiveness of sea floor mapping could be increased (Purser et al., 2018).

For accurate measurement of underwater distances, traditional visual techniques are often compromised by factors such as scattering and feature degradation in marine environments. Zhang et al. (2024) introduced an innovative methodology that integrates image sonar with stereo vision, thereby enhancing visual feature detection. By implementing a novel sonar-based cost term, this approach not only improves precision of depth estimations but also enhances texture details within depth maps.
Imaging sonars and optical cameras were compared for estimating fish densities at artificial reefs. This study analysed fish assemblage data acquired using imaging sonars operating at four frequencies (0.75, 1.2, 2.1, and 3 MHz) alongside simultaneous optical camera footage at two artificial reefs. The results indicated that fish densities recorded by sonar were, on average, three times greater than those observed through optical methods (Sibley et al., 2023).

The studies mentioned above show some potential applications for the combined use of sonar and underwater cameras and demonstrate how diverse the possibilities are. We believe that these technologies can complement each other in terms of underwater surveying, ideally by photogrammetrically created 3D point clouds from the camera data for more detailed analysis. Even when point clouds are not possible (because of turbid water), the camera data can be a valuable addition, as this experiment shows.

2. Methods and Results

2.1 Imaging Sonar characteristics

The Oculus M3000d imaging sonar used for this study is equipped with 1.2 MHz and 3 MHz frequencies (Blueprint, 2025). More details are shown in Table 1. In this study, the sonar was mostly used with the 1.2 MHz frequency setting, due to its longer range. Also, the better spatial orientation was an advantage for the ROV pilot.

Sonar Frequency / MHz	Horizontal coverage / degrees	Vertical beamwidth / degrees	Max range available / m
1.2	130	20	30
3	40	20	5

Table 1. The beam geometry characteristics of the different imaging sonar systems available in this study. (Blueprint. 2025)

2.2 Data collection

In the first step, we had to find the barrels in an area of over 1 ha. The imaging sonar was used for finding the barrel; by using this method we were able to locate twelve barrels in the pond. In Figure 1, a representative barrel is shown as it was seen through the imaging sonar. The barrels were inspected with the sonar and the camera, the low visibility limited the options of photogrammetric evaluation drastically. We realized that it is not feasible to create a photogrammetric 3D point cloud to determine the dimensions of the barrels. To answer the second research questions and determine the dimensions of the barrel, we decided to use the imaging sonar in the first step.

2.3 Determining the height of the barrels

We extracted the height of the barrels directly from the imaging sonar data. In Figure 1–5, one can see how the height of the barrel was measured in the program “Oculus Viewpoint” using the multibeam sonar recordings. The barrels were recorded from different angles, which can also be seen in the Figures 1–5. One can see that in all cases, the measured height is close to the reference value, independent of the sonar range and the angle between the imaging sonar and the object. Table 2 shows the results of ten separate height measurements of the barrels that were conducted using data from the imaging sonar.

By comparing these results with the known reference value (Table 4), we calculated the error of the mean value which corresponds to 3.5%. This result could be achieved from several meters distance.

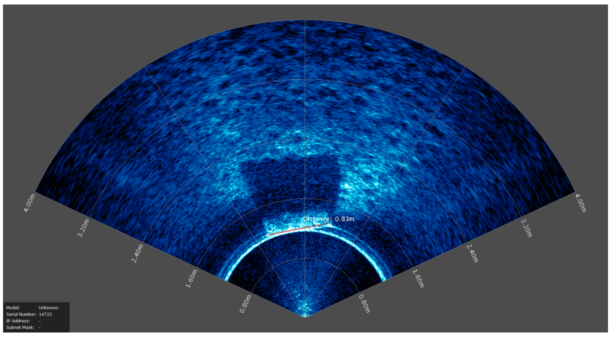

Figure 1. Barrel seen through the imaging sonar.
Measured height: 83 cm.

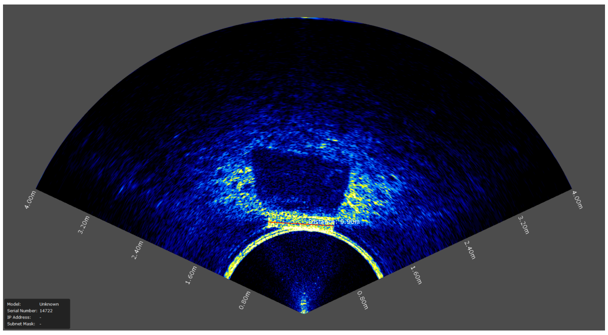

Figure 2. Barrel seen through the imaging sonar.
Measured height: 90 cm.

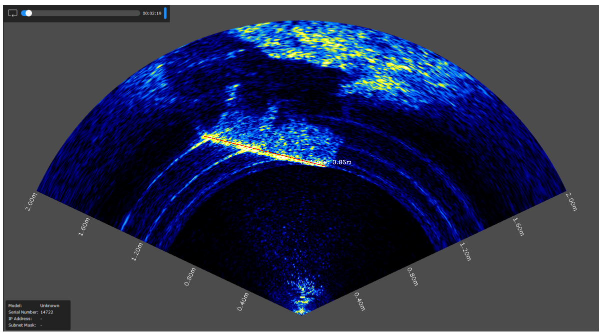

Figure 3. Barrel seen through the imaging sonar.
Measured height: 86 cm.

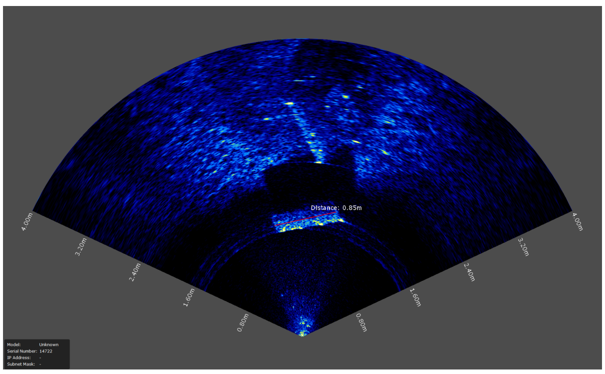

Figure 4. Barrel seen through the imaging sonar.
Measured height: 85 cm.

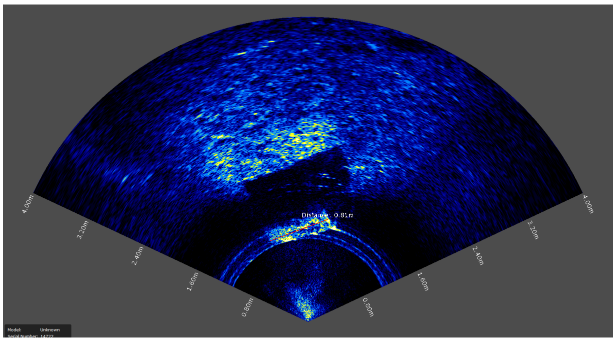

Figure 5. Barrel seen through the imaging sonar.
Measured height: 81 cm.

Number	Height / m	Error / m
1	0.83	0.03
2	0.77	0.09
3	0.85	0.01
4	0.85	0.01
5	0.79	0.07
6	0.78	0.08
7	0.9	0.04
8	0.86	0.00
9	0.82	0.04
10	0.82	0.04
Mean	0.83	0.03
Std. Dev.	0.04	-

Table 2. Height of the barrel measured using the imaging sonar.

2.4 Determining the barrel diameter

In the next step, we derived the diameter of the barrel. As we showed in Table 4, the reference value is 61cm. For the extraction of the barrel's diameter we used different methods, combining the use of three different sensors, the imaging sonar, the camera, and the laser scaler.

2.4.1 Determining the barrel diameter by using the imaging sonar: In a first approach, we used the data recorded with the imaging sonar. In Table 3, results of five different measurements are shown. The results for the barrel diameter are not close to the reference diameter. The error of the mean diameter is 0.21 m or 34% of the reference value. By taking a closer look at Table 3, we can see that each single measurement differs significantly when compared to the reference diameter.

This results in a smaller diameter on the imaging sonar and the operator has no real chance to realize this, if the diameter is not known beforehand. The sonar was able to accurately determine the height of the barrels, but it did not work with satisfactory accuracy for the barrel diameter, even assuming that millimeter accuracy was not required.

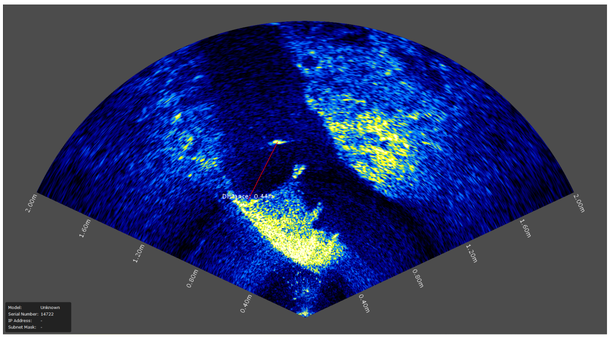

Figure 6. Barrel seen through the imaging sonar.
Measured diameter: 44 cm.

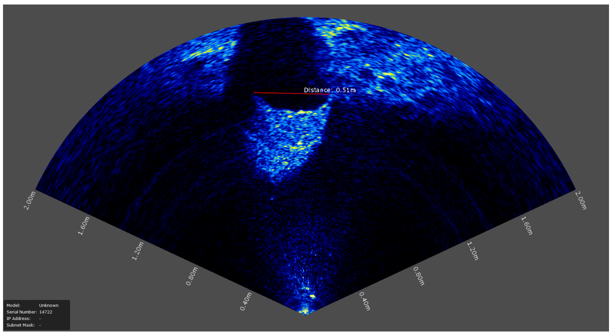

Figure 7. Barrel seen through the imaging sonar.
Measured diameter: 51 cm.

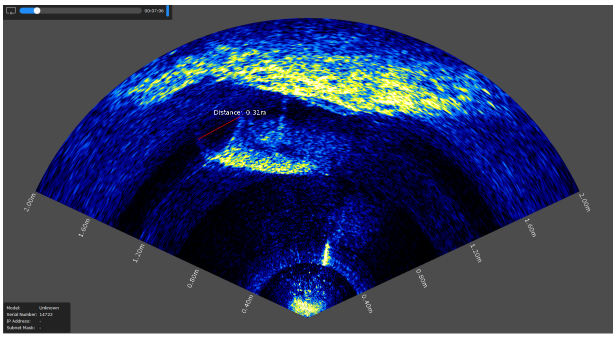

Figure 8. Barrel seen through the imaging sonar.
Measured diameter: 32 cm.

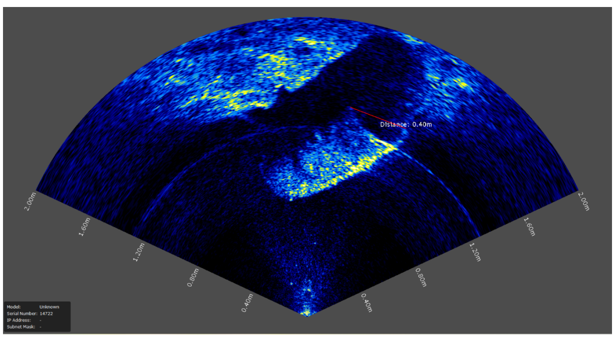

Figure 9. Barrel seen through the imaging sonar.
Measured diameter: 40 cm.

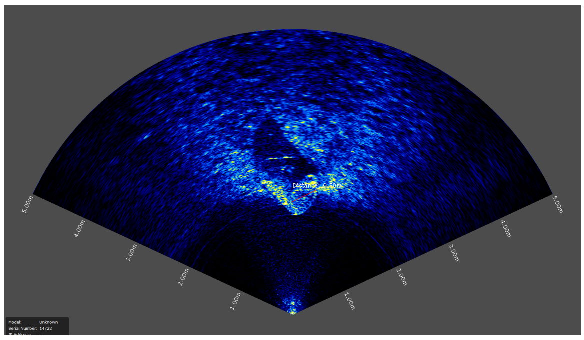

Figure 10. Barrel seen through the imaging sonar.
Measured diameter: 50 cm.

Number	Measured Diameter / m	Error / m
1	0.68	0.07
2	0.36	0.25
3	0.57	0.04
4	0.31	0.30
5	0.28	0.33
6	0.44	-0.17
7	0.33	-0.28
8	0.45	-0.16
9	0.32	-0.29
10	0.4	-0.21
Mean	0.41	0.21
Std. Dev.	0.12	-

Table 3. Diameter of the barrel measured using the imaging sonar.

Reference Barrel Height	0.86 m
Reference Barrel Diameter	0.61 m

Table 4. Reference dimensions of the barrels.

In Figures 6–10, we showed how the diameter of the barrel looked like on the imaging sonar. The images demonstrate that it is not intuitively noticeable, that only a part of the diameter is shown in the imaging sonar. To us, it looked like the whole barrel was visible, and only after comparing it to the reference diameter, we noted the discrepancy. The error of the barrel diameter measured from the imaging sonar exhibits reasonable standards.

2.4.2 Determining the barrel diameter by using the camera and laser scaler: Consequently, we had to use a different sensor to determine the diameter of the barrels, namely the camera in combination with the laser scaler. While the camera was limited by the high turbidity of the water, by getting closer to the object without disturbing the muddy floor and raising any particles, we could take a relatively clear picture of the barrel top. The picture is shown in Figure 11. The laser scaler (two red dots) has 10 cm distance and is used to scale the pixels. With this information, we could determine the parameters necessary for the following calculation.

Method 1: To estimate the barrel diameter, we used the circular segment to calculate the parameters h (sagitta) and s (chord length), which are also drawn into the image. Using formula (1), we received a diameter of 0.62 m, which is close to the reference diameter of 0.61 m. This motivated us to further investigate this method for obtaining the diameter.

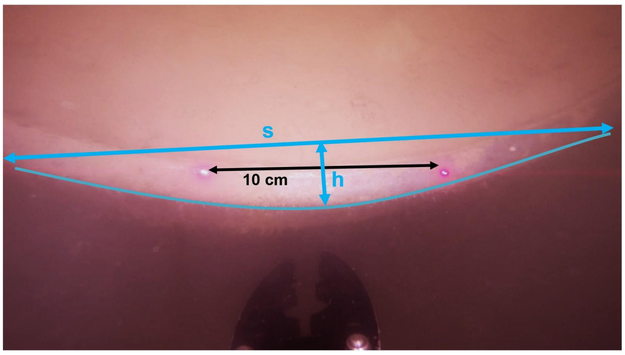

Figure 11. Part of the barrel seen in the camera. The parameters of formula (1) are highlighted in the figure.

$$d = \frac{4h^2 - s^2}{4h} \quad (1)$$

where d = diameter
s = chord length
h = sagitta

Method 2: Another simple way to obtain the barrel diameter using the picture of the barrel is by drawing a full circle into the circle segment. This is shown in Figure 12. By comparing the pixels between the two laser dots with the diameter of the drawn circle, one can obtain the searched diameter. This method resulted in a diameter of 60 cm.

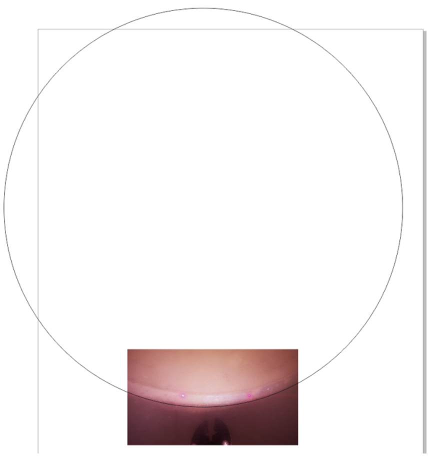

Figure 12. The diameter can also be determined graphically by drawing a circle that fits the segment.

	Calculated Barrel Diameter / m	Reference Barrel Diameter / m	Error / m
Imaging Sonar	0.41	0.61	0.21
Method 1	0.62	0.61	0.01
Method 2	0.60	0.61	0.01

Table 5. Calculated barrel diameter from the camera image using Method 1 and Method 2.

In Table 5, the calculated barrel diameter using the three different methods, are shown. Both image-based methods have a deviation of 1 cm, a large improvement compared to the error of 20 cm that was obtained using the imaging sonar.

3. Conclusion and Outlook

We used a ROV and a combination of three sensors (imaging sonar, camera, laser scaler) to locate twelve industry oil barrels in a pond and to determine the dimensions of these barrels. Combinations of these sensors proved to be useful. The imaging sonar worked well to locate the barrels and determine its height, and the camera was used to calculate the barrel diameter. Sonar in general and imaging sonar particular can play a crucial role in underwater infrastructure inspection (Agnisarman et al., 2019). The combination of sonar data with photogrammetry can increase the quality of the results (Cooper et al., 2023)

The combination of the three sensors: imaging sonar, camera, and laser scaler enabled us to determine the height and the diameter of the barrels in the pond. The imaging sonar was used to determine the height of the barrels, a task that could not be done with the camera because of the high turbidity. There is an uncertainty in measuring the barrels with the imaging sonar, however after taking the mean value of 10 measurements the error was reduced to 3,5 %. The diameter of the barrels could not be measured correctly using the sonar data, the error was 33%. Some of the measured values (Table 2, Number 2, 4, 5, 7, 9) are incorrect, because the barrel was partially submerged into the muddy ground, and therefore only a part of the diameter was visible in the imaging sonar data. In a second approach, using the camera and laser data, we could derive the barrel diameter with an error of only 1.6 %.

The use of different sonar frequencies could increase the accuracy. By measuring the length of fish with different sonar frequencies, it was demonstrated that the accuracy of length measurements made using imaging sonar is inversely proportional to the beamwidth (Parnum et al., 2019). As we showed in Table 1, the higher frequency setting has a lower bandwidth and therefore a higher accuracy is possible.

In future work, we will employ more techniques to calculate the barrel diameter using the optical camera and compare them to choose the option with the highest accuracy. We aim at identifying an option that works for many different shapes and sizes of objects.

References

Agnisarman, S., Lopes, S., Madathil, K. C., Piratla, K., Gramopadhye, A., 2019. A survey of automation-enabled human-in-the-loop systems for infrastructure visual inspection. *Automation in Construction*, 97, 52-76.

Blueprint, 2025. Blueprint Oculus M-series specifications. https://www. blueprintsubsea.com/oculus/oculus-m-series (10 June 2025).

Cardaillac, A., Ludvigsen, M., 2023. Camera-sonar combination for improved underwater localization and mapping. *IEEE Access*, 11, 123070-123079.

Chemisky, B., Nocerino, E., Menna, F., Nawaf, M. M., and Drap, P., 2021. A portable opto-acoustic survey solution for mapping of underwater targets, *International Archives of Photogrammetry, Remote Sensing and Spatial Information Sciences*, XLIII-B2-2021, 651–658.

Cook, D., Middlemiss, K., Jaksons, P., Davison, W., Jerrett, A., 2019. Validation of fish length estimations from a high frequency multi-beam sonar (ARIS) and its utilisation as a field-based measurement technique. *Fisheries research*, 218, 59-68.

Cooper, I., Hotchkiss, R. H., Williams, G. P., 2020. Extending Multi-Beam Sonar with Structure from Motion Data of Shorelines for Complete Pool Bathymetry of Reservoirs. *Remote Sensing*, 13(1), 35.

Deeptrekker, 2025. Revolution series specifications. https://www.deeptrekker.com/shop/products/revolution-x-rov (1 June 2017)

Demer, D.A., Berger, L., Bernasconi, M., Bethke, E., Boswell, K., Chu, D., Domokos, R. et al., 2015. Calibration of acoustic instruments. ICES Cooperative Research Report No. 326, 133. DOI: http://dx.doi.org/10.25607/OBP-185

Helminen, J., Dauphin, G. J., Linnansaari, T., 2020. Length measurement accuracy of adaptive resolution imaging sonar and a predictive model to assess adult Atlantic salmon (Salmo salar) into two size categories with long-range data in a river. *Journal of fish biology*, 97(4), 1009-1026.

Helminen, J., Linnansaari, T., 2023. Combining imaging sonar counting and underwater camera species apportioning to estimate the number of Atlantic salmon and striped bass in the Miramichi River, New Brunswick, Canada. *North American Journal of Fisheries Management*, 43(3), 743-757.

Lurton, X., 2010. *An introduction to underwater acoustics: Principles and applications.* 2nd ed., Berlin, Heidelberg, Springer.

Parnum, I. M., Saunders, B. J., Stott, M., Elsdon, T. S., Marnane, M. J., Harvey, E. S., 2024. The accuracy of length measurements made using imaging SONAR is inversely proportional to the beamwidth. *Methods in Ecology and Evolution*, 15(5), 824-835.

Purser, A.., Marcon, Y.., Dreutter, S.., Hoge, U.., Sablotny, B., Hehemann, L.., Lemburg, J.., Dorschel, B.., Biebow, H., Boetius, A., 2018: Ocean Floor Observation and Bathymetry System (OFOBS): A new Towed Camera/Sonar System for Deep-Sea Habitat Surveys, *IEEE Journal of Oceanic Engineering*, 44(1), 87-99.

Sibley, E. C. P., Elsdon, T. S., Marnane, M. J., Madgett, A. S., Harvey, E. S., Cornulier, T., Driessen, D., & Fernandes, P. G., 2023. Sound sees more: A comparison of imaging sonars and optical cameras for estimating fish densities at artificial reefs. *Fisheries Research*, 264, Article 106720.

Song, Y. E., Choi, S. J., 2016. Underwater 3D reconstruction for underwater construction robot based on 2D multibeam imaging sonar. *Journal of Ocean Engineering and Technology*, 30(3), 227-233.

Sun, K., Cui, W., Chen, C., 2021. Review of underwater sensing technologies and applications. *Sensors*, 21(23), 7849.

Sun, W., Hou, S., Wu, G., Zhang, Y., & Zhao, L., 2025. Two-step rapid inspection of underwater concrete bridge structures combining sonar, camera, and deep learning. *Computer-Aided Civil and Infrastructure Engineering*, 1–21.

Wei, Y., Duan, Y., An, D., 2022. Monitoring fish using imaging sonar: Capacity, challenges and future perspective. *Fish and Fisheries*, 23(6), 1347-1370.

Zhang, J., Han, F., Han, D., Yang, J., Zhao, W., Li, H., 2024. Advanced underwater measurement system for ROVs: integrating sonar and stereo vision for enhanced subsea infrastructure maintenance. *Journal of Marine Science and Engineering*, 12(2), 306.

https://doi.org/10.5194/isprs-archives-XLVIII-2-W10-2025-95-2025